Journal of Applied Research and Technology

www.jart.icat.unam.mx

Instituto de Ciencias Aplicadas y Tecnología

Journal of Applied Research and Technology 24 (2026) 553-563

Original

Modelling the Influence of Nano-Additives and Generic Chemical Reaction on Thermo-migration in High Speed Magnetohydrodynamic Stream Drift

Uchenna Awucha Uka*[1] • Edwin Esekhaigbe[2]
Digbo Idika Iku[2] • Alex Musa[3]

[1]Department of Basic Sciences, School of Science and Technology,
Babcock University, Ogun State, Nigeria
[2]Department of Mathematics and Computer Science,
University of Africa, Bayelsa State, Nigeria
[2]Department of Basic Sciences, School of Science and Technology,
Babcock University, Ogun State, Nigeria
[3]Departmentment of Mathematics and Statistics,
University of Port Harcourt, Port Harcourt, Nigeria

Received: 03 12 2024; Accepted: 10 07 2025
Available: 31 08 2026

Abstract: The investigation models a steady free convective flow generated by a vertically stretched and shielded sheet moving through a thermo-migration induced by high-speed stream drift. A boundary layer approximation establishes a well-posed mathematical model encompassing momentum, energy, and mass equations. The leading partial differential models (PDMs) were meticulously transformed into nonlinear coupled ordinary differential models (ODMs) using a balanced non-similar transformation approach to facilitate a successful numerical solution. The numerical solution involves the application of proficient schemes, named the fourth-order Runge-Kutta-Fehlberg approach and shooting technique, implemented with MAPLE V.10. The velocity, temperature, and concentration profiles are presented, and they highlight the influence of various pertinent fluidic parameters. The impact of chaotic motion induced by finely divided conducting nano-additives in the fluid is also investigated. It was found that surface conditions

*Corresponding author.
E-mail address: ukau@babcock.edu.ng (I. Mendoza-Bravo).
Peer Review under the responsibility of Universidad Nacional Autónoma de México.

influence velocity reduction. The findings demonstrate that an increase in thermo-migration begets elevated velocity and energy but a diminishing trend in diffusivity. Furthermore, the strengthening of the magnetic field induces a velocity reduction, just as the magnetohydrodynamic effects alter fluid dynamics in reaction systems. Additionally, the Hartmann number disrupts thermal boundary layer development, leading to a reduction in the local heat transport and skin-friction coefficient. Thus, the practical applications of the results of this study will be beneficial to several manufacturing, processing, transportation, and automobile industries.

Keywords: **Boundary constraints, mass diffusivity, RGK 4th order, shooting scheme, thermal control**

1. Introduction

Heat and mass transfer are integral to diverse industrial applications such as power generation, chemical processing, and aerospace engineering. In these processes involving fluid movement, understanding the thermal and mass transmission characteristics is vital for enhancing the efficiency and performance of procedures. Magnetohydrodynamic (MHD) fluid drift specifically involves a conductive fluid strongly interacting with magnetic fields. The fluid's motion, in contact with the electromagnetic field, is governed by the Lorentz force, influencing the behavior of charged particles, typically electrons and ions, within the MHD fluid. The key characteristics of MHD fluids encompass:

a. Conductivity: MHD fluids exhibit heightened electrical conductivity, facilitating the conduction of electric currents.

b. Interaction with magnetic fields: Fluid motion induces electric currents, leading to the generation of magnetic fields. The interplay between existing and induced magnetic fields significantly influences fluid flow.

c. Lorentz Force: Arising from the interaction between the magnetic field and electric current in the fluid, the Lorentz force can impact fluid movement, giving rise to unique phenomena like the generation of electric currents and magnetic fields within the fluid. MHD flows have been extensively studied due to their potential applications in various fields such as nuclear reactors, space propulsion, and materials science. The study emphasizes the importance of thermo-migration and generic chemical reactions. Thermo-migration involves the movement of particles within a substance in response to temperature gradients, observed in fields like materials science and fluid dynamics. This phenomenon is particularly relevant in nanomaterials and microscale systems, influencing the redistribution of particles and affecting overall material properties. Understanding thermo-migration is crucial for designing and optimizing materials, especially in electronic devices where temperature differentials impact performance. Generic chemical reactions, representing transformations without specifying exact reactants and products, offer a generalized approach. This method is valuable when specific chemical species are not pivotal to the analysis, or when the goal is to understand broader trends and behaviors in a system. Such reactions find applications in diverse fields, including chemical engineering, environmental science, and theoretical chemistry, aiding in model development, exploring reaction pathways, and understanding fundamental principles governing chemical transformations without being constrained to specific chemical compositions. In recent times, numerous scholars have delved into the characteristics of heat and mass transfer in MHD flows. One study (Krishna et al., 2023) focused on the non-steady MHD natural convection past an exponential plate immersed in a permeable material, examining the Hall and ion slip impacts using the Laplace transformation method, and found that a disposition angle prevents a decrease in velocity. Another investigation explored the electromagnetic hydrodynamic convective drift of an electrically propelling viscous liquid with wall suction and Joule heating effects (Wakif et al., 2020). Utilizing generalized differential quadrature and Newton-Raphson iterative approaches, the study observed that wall suction enhances thermal allocation speed near the Riga plate. In a related development, researchers (Krishna et al., 2020) studied the Hall and ion effects in a non-steady laminar MHD convective rotating fluid flow past an unbounded half-upright stirring leaky object. Applying perturbation techniques, the study revealed that increasing Hall and ion parameters leads to a rise in velocity. The Reiner-Philippoff liquid flow over a heated external wall with thermal diffusivity was examined (Kumar et al., 2019) using the Runge-Kutta-Fellberg (RKF-45) technique, indicating a greater decrease in heat transfer for pseudo-plastic liquid compared to other fluids. The simulation of hydromagnetic nano-liquid flow over an inclined fiery plate with non-uniform thermal generation/absorption and radiation was scrutinized (Uka et al., 2022) by applying regular perturbation and a Mathematica package. Results indicated a decrease in velocity with an increase in inclination angle, while an enhancement of the energy reliance non-uniform number led to an increase in heat transportation speed. The investigation of heat radiative effects on MHD immobility fluid past an elastic material with slip wall settings, using an inbuilt MATLAB solver to find that the heat wall layer thickness shrinks with rising Grashof and Prandtl parameters has been reported (Raptis, 2017). Another study examined the joint influence of heat and mass diffusion on the free convective unsteady MHD stream of micropolar fluid immersed in an absorbent material, utilizing the Laplace transform technique (Farhad et al., 2013). Results revealed that velocity improves with increasing porosity and Grashof factors but decreases for higher values of M and $Pr > 1$. Additionally, an investigation on Soret and Dufour impacts on MHD unsteady liquid stream past a moving superimposed upright sheet through thermal radiation and heat production (Bejawada & Yanda, 2021) utilized the Galerkin finite element procedure, finding that an increase in the Soret number indicates a rise in concentration, while skin friction decreases with higher Soret and Dufour factors. Finally, (Kasmani et al., 2016) explored the influence of radiation on MHD drift across an optically thin grim fluid within a vertical absorbent medium using the shooting process, determining that velocity is enhanced due to increased radiation and Grashof constraints. Certain studies suggest that nano-fluids exhibit superior thermal conductivity compared to traditional fluids. For instance, in a study by (Shahzad et al., 2021) a two-dimensional, non-compressible Jeffrey thermal transfer fluid flow with an elastic wall was considered. The researchers utilized the Keller-Box methodology for numerical solutions, revealing that nanoparticle concentration and the magnetic field reduce shear stress, while the rate of heat movement increases on the wall due to Deborah's parameter. Another investigation employed the Galerkin finite element technique to analyze a combined convective TiO2-SiO2/water mix nanoliquid stream past a three-sided opening frenzied base (Radouane et al., 2021). Results indicated that the Hartmann number has little effect on both velocity and heat distributions. In a study (Jamshed et al., 2020), the numerical impact of a magnetized energetic Powell-Eyring nanofluid with a one-segment model was deliberated using the Keller Box approach. The researchers noted that the heat conductance in Powell-Eyring fluid continuously intensifies, unlike orthodox fluid. Examining the influence of heat generation on a non-steady MHD natural convection drift involving Casson liquid over an upright wavering sheet in the presence of leaky material (Goud et al., 2020), the finite element tool was employed to recover the solution. The findings revealed that an increase in the thermal base number boosts the fluid's velocity and temperature. The impact of a disposed magnetic field on momentum, thermal, and mass relocation with Williamson nanofluid above an elastic plate was investigated (Srinivasulu & Goud, 2020). The numerical resolution involved Runge-Kutta-Fehlberg's fourth-fifth and shooting schemes, unveiling that a higher value of magnetic and inclination angle factors raises velocity, temperature, and concentration, while the Williamson number reduces the speed of thermal transmission. Additionally, (Shankar et al., 2020) explored the radiation impact on MHD boundary layer flow past a stretchy plate using the MATLAB solver bvp5c scheme. Their findings indicated a decline in heat transfer at the wall due to increased parametric values of magnetic strength and radiation. The Homotopy Analysis Method (HAM) was employed in another study (Animasaun et al., 2016) to investigate Casson fluid flow characterized by variable thermo-physical properties along an exponentially stretching sheet. This study considered the effects of suction and exponentially decaying internal heat generation, highlighting that an increase in the variable plastic dynamic viscosity number led to a surge in velocity distribution and a decline in temperature throughout the boundary layer.

This research is highly relevant to energy conversion systems and material processing applications, where efficient heat and mass transfer are paramount. The presence of a magnetic field in MHD fluids can substantially influence heat and mass transfer characteristics. Therefore, understanding this influence is crucial for advancing the design and operational efficiency of MHD-based systems. The primary objective of this study is to investigate how nano-additives and chemical reactions affect thermo-migration in high-speed MHD fluid flow. The research encompasses several aspects, including modeling the physical flow configuration, converting these models into coupled nonlinear ordinary differential equations (ODEs), implementing numerical schemes to solve the problem based on influential fluid parameters, and presenting the results in tables and graphs. The anticipated outcomes of this study are expected to provide insights into fundamental mechanisms in engineering and materials science, paving the way for potential advancements, improvements, and optimization processes.

2. Mathematical Formulation

We examine the behavior of a laminar, steady, two-dimensional, viscous, incompressible, and electrically conductive high-speed MHD fluid influenced by thermo-migration and generic chemical reaction rates as it flows past a vertically stretched surface. Fluid dynamics involve the passage of fluid over a porous material experiencing high-speed motion, with applications in various industrial scenarios such as heat exchangers, chemical reactors, and cooling systems. The initial flow position is at $x = 0$, with the $x - axis$ aligned along the flow direction v, and the perpendicular direction u along the $y - axis$. The induced magnetic Reynolds number, $Re \ll 1$, suggests that the impact of the Lorentz force on the fluid, resulting from the applied magnetic strength, is negligible. Consequently, its influence on the flow is not significant. However, the strength of the applied magnetic field becomes crucial as the fluid becomes magnetized and interacts with the magnetic field, introducing effects on velocity, among other parameters. The physical geometry of the flow is illustrated in Figure 1.

Similarly, the mathematical models for the fluid problem are stated below, (Boussinesq, 1877).

Continuity equation:

$$\frac{\partial}{\partial x}(ru) + \frac{\partial}{\partial y}(rv) = 0 \tag{1}$$

Momentum conservation equation:

$$u\frac{\partial u}{\partial x} + v\frac{\partial u}{\partial y} = -\frac{1}{\rho}\frac{\partial p}{\partial x} + v\frac{\partial^2 u}{\partial y^2} - \frac{\sigma B_o^2}{\rho}u + g\alpha(T - T_\infty) + g\alpha(C - C_\infty) - \frac{v}{\lambda}\Omega u \tag{2}$$

Energy transport equation:

$$(ru)\frac{\partial T}{\partial x} + (rv)\frac{\partial T}{\partial y} = \beta_m\frac{\partial^2 T}{\partial y^2} - \frac{\Omega}{\rho C_p}\frac{\partial q_r}{\partial y} + \tau\left[D_T\frac{\partial T}{\partial y}\frac{\partial \emptyset}{\partial y} + \frac{D_T}{T_\infty}\left(\frac{\partial T}{\partial y}\right)^2\right] + \frac{Q_h}{\rho C_p}(T - T_\infty) \tag{3}$$

Diffusion equation:

$$u\frac{\partial \emptyset}{\partial x} + v\frac{\partial \emptyset}{\partial y} = D\frac{\partial^2 \emptyset}{\partial y^2} + \left(\frac{D_T}{T_\infty}\right)\frac{\partial^2 T}{\partial y^2} - \omega(C - C_\infty) \tag{4}$$

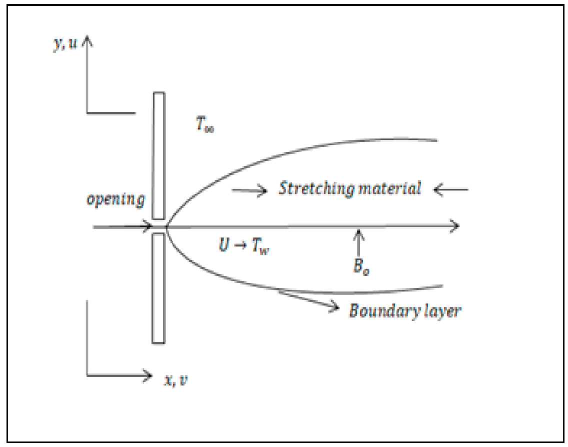

Figure 1. Flow configuration with coordinates

Under the boundary constraints arranged as:

$$\begin{gathered} v = 0,\ T = T_w,\ \emptyset = \emptyset_w \text{ at } y = 0 \\ u = v \to 0,\ T \to T_\infty,\ \emptyset \to \emptyset_\infty \text{ as } y \to \infty \end{gathered} \tag{5}$$

With

$$\alpha, \Omega, g, \lambda, \beta_m, \rho_f, q_r, \tau, D, D_T, \omega, Q_h, T, C, T_\infty, C_\infty$$

signifying convectional fluid volumetric intensifying factor, absorbency, acceleration with gravity, the porousness of the medium, the ratio of the thermal diffusivity to specific heat capacity, fluid density, heat flux, the ratio of thermal strength of fluid to nanoparticle, random motion number, thermophoresis coefficient, chemical reaction influence, heat term, local temperature and concentration, temperature, and concentration away from the wall, respectively. More so, the second term on the right-hand side (RHS) of Eq. (3) refers to heat change owing to radiation. The dimensionless temperature and nano-additives volume fraction are prescribed as:

$$\begin{gathered} T - T_\infty = \theta(t)(T_w - T_\infty) \\ C - C_\infty = \emptyset(\eta)(C_w - C_\infty) \end{gathered} \tag{6}$$

3. Materials and Methods

The similarity transformational variables are defined in the following order.

$$\psi(x, y) = f(\eta)\sqrt{U_\infty v x},\ \eta = \left(\frac{y}{x}\right)(Re_x)^{\frac{1}{2}} = y\left(\frac{U_\infty}{vx}\right)^{\frac{1}{2}} \tag{7}$$

$$u = \frac{1}{r}\frac{\partial \psi}{\partial y},\ v = -\frac{1}{r}\frac{\partial \psi}{\partial x} \tag{8}$$

Meanwhile, from the estimation below (Rosseland, 1936), we have,

$$\mathrm{qr} = -\frac{4\sigma_s \partial T^4}{3k_q \partial y} \tag{9}$$

Where,

Q_s, k_q implies the Stefan-Boltzmann and mean absorption numbers. Therefore, it is pertinent to state that when the temperature variance around the flow becomes minimal, the expansion of T^4 ensues, and this is carried out by using Taylor's series extension about T_∞ . Hence, by deserting terms of a greater degree than the first degree in (T - T_∞) we obtained the following:

$$T^4 \approx 4T_\infty^3 - 3T_\infty^4 \tag{10}$$

Putting Eq. (10) into Eq. (9) and simplifying yields:

$$\frac{\partial \mathrm{qr}}{\partial y} = \frac{\partial}{\partial y}\left(-\frac{16T_\infty^3\sigma^*}{3k^*}\frac{\partial T}{\partial y}\right) \tag{11}$$

Using Equation (11) in Eq. (3), gives:

$$\begin{aligned}(\mathrm{ru})\frac{\partial T}{\partial x} + (\mathrm{rv})\frac{\partial T}{\partial y} = \beta_m \frac{\partial^2 T}{\partial y^2} - \frac{\partial}{\partial y}\left(-\frac{16T_\infty^3\sigma^*\Omega}{3k^*\rho C_p}\frac{\partial T}{\partial y}\right) + \\ \frac{Q_h}{\rho C_p}(T - T_\infty) + \tau\left[D\frac{\partial T}{\partial y}\frac{\partial \emptyset}{\partial y} + \frac{D_T}{T_\infty}\left(\frac{\partial T}{\partial y}\right)^2\right]\end{aligned} \tag{12}$$

However, Eq. (1) is satisfied upon substituting Eq. (8) into it. Thus, putting Eqs. (6)–(8) into Eqs. (2), (4), and (12), and simplifying them, reduces to:

$$\begin{aligned}f'''(\eta) + \tfrac{1}{2}f(\eta)f''(\eta) - Hf'(\eta) + \\ Gr\theta(\eta) + Gn\emptyset(\eta) - \beta f'(\eta) = 0\end{aligned} \tag{13}$$

$$\begin{aligned}\theta''(\eta)\left(1 + \tfrac{4}{3}S\right) + Pr\left[f'(\eta)\theta(\eta) + f(\eta)\theta'(\eta)\right] + \\ Nb\theta'(\eta)\emptyset'(\eta) + Nr(\theta')^2(\eta) + K_h\theta(\eta) = 0\end{aligned} \tag{14}$$

$$\emptyset''(\eta) + Scf(\eta)\emptyset'(\eta) + \frac{Nb}{Nr}\theta''(\eta) - Cr\emptyset(\eta) = 0 \tag{15}$$

The resultant transformed conditions at the boundary are indicated as follows.

$$\begin{aligned}f(0) = 0, f'(0) = 1, \theta(0) = 1, \emptyset(0) = 1, \\ f'(\infty) = 0, \theta(\infty) = 0, \emptyset(\infty) = 0\end{aligned} \tag{16}$$

The physical dimensionless quantities of interest in Equations (12)–(14) include:

$$\begin{aligned}&H = \frac{\sigma B_0^2 x}{\rho U_\infty},\ Gr = \frac{g\alpha(T_w - T_\infty)x}{U_\infty^2},\ Gn = \frac{g\alpha(C_w - C_\infty)x}{U_\infty^2}, \\ &\beta = \frac{\mu\Omega x}{\lambda U_\infty},\ S = \frac{4T_\infty^3\sigma^*\Omega}{k^*\beta\rho C_p},\ Pr = \frac{\vartheta U_\infty}{2\beta x},\ k_h = \frac{Q_h}{\rho C_p}, \\ &Nb = \frac{\tau U_\infty D(C_w - C_\infty)}{T_\infty v x},\ Nr = \frac{\tau U_\infty D_T(T_w - T_\infty)}{vx},\ Sc = \frac{v}{D}, \\ &Cr = \frac{\omega v x}{D U_\infty}\end{aligned} \tag{17}$$

The dimensionless parameters in Equation (17) are defined as modified Hartmann factor, local thermal and mass Grashof numbers, surface condition parameter, radiation, Prandtl, optimized heat source number, pedesis parameter, thermo-migration number, Schmidt, and reformed generic chemical reaction rate parameters, respectively. However, the vital quantities of practical reputation in the engineering field include the skin friction coefficient C_f, Nusselt Nu_x, and Sherwood Sh_x numbers defined as follows:

$$\begin{aligned}C_f &= \frac{\mu}{\rho u_w^2}\left(\frac{\partial u}{\partial y}\right)_{y=o} \\ Nu_x &= \frac{xq_w}{k(T_w - T_\infty)} \\ Sh_x &= \frac{xq_m}{D(C_w - C_\infty)}\end{aligned} \tag{18}$$

With the heat conductance of the nano-liquid represented by k, and:

$$\begin{aligned}q_w &= -\left(\frac{\partial T}{\partial y}\right)_{y=0} \\ q_m &= -D\left(\frac{\partial C}{\partial y}\right)_{y=0}\end{aligned} \tag{19}$$

Putting Equation (10) into Equation (17) produces:

$$\begin{aligned}f''(0) &= \sqrt{Re_X}C_f \\ -\theta'(0) &= \frac{Nu_x}{\sqrt{Re_X}} \\ -\emptyset'(0) &= \frac{Sh_x}{\sqrt{Re_X}}\end{aligned} \tag{20}$$

with the local Reynolds term $Re_X = \frac{U_\infty x}{v}$.

The application of the Runge-Kutta-Fehlberg fourth order with the shooting scheme is utilized to solve the set of nonlinear differential equations (NDEs) and boundary value problems from Equations (13)–(15) with the boundary constraints (16). Therefore, through the aid of transformational variables, the equations mentioned above, subject to Equation (16), are transformed into a system of first-order ODEs as stated below, with the appropriate boundary conditions.

$$\begin{aligned}f = h_1, f' = h_2, f'' = h_3, f''' = hh_1 \\ hh_1 = -\tfrac{1}{2}h_1h_3 + Hh_2 - Grh_4 - Gnh_6 + \beta h_2\end{aligned} \tag{21}$$

$$\begin{aligned}\theta = h_4, \theta' = h_5, \theta'' = hh_2 \\ hh_2 = -\frac{1}{\left(1+\frac{4}{3}S\right)}\left[Prh_2h_4 + h_1h_5 + Nbh_5h_7 + Nr(h_5)^2 + k_hh_4\right]\end{aligned} \tag{22}$$

$$\begin{aligned}\emptyset = h_6, \emptyset' = h_7, \emptyset'' = hh_3 \\ hh_3 = -\left[Sch_1h_7 + \frac{Nb}{Nr}hh_2 - Crh_6\right]\end{aligned} \tag{23}$$

The corresponding boundary constraints include:

$$h_1(0) = 0,\ h_2(0) = 1,,h_4(0) = 1,\ h_6(0) = 1$$
$$h_2 \to 0,\ h_4 \to 0,\ 6 \to 0 \text{ as } \eta \to \infty \tag{24}$$

The following steps have been applied in solving the problem. The set of converted nonlinear first-order differential Equations (NFODEs) (21)–(23) aligned with Equation (24) is numerically resolved by adopting a shooting scheme with an in-built Runge-Kutta Fehlberg integration algorithm. The nonlinear problem is clearly defined and expressed as a system of first-order ODEs of the form, . The boundary conditions for the problem, which specify the values of the solution at the endpoints of the interval, are stated. This approach entails changing Equations (13)–(15) into initial value problems, which are to be solved by the initial guessing approach, while a Runge-Kutta-Fehlberg integration algorithm is engaged to integrate Equations (21)–(23) with Equation (24) repeatedly, pending when the prescribed boundary constraints are satisfied within a specified tolerance. Thus, the computational technique was executed by applying the MAPLE solver scheme. Meanwhile, all the simulations were computed with the parametric values $Pr = 0.71$, $Cr = 1.0$, $Gr = 3.0$, $H = S = Nb = Nr = Sc = k_h = 0.5$.

4. Results and Conclusion

The results depict distributions of velocity, temperature, and nano-additive species concentration, along with tables presenting the effect of a key parameter on the skin-friction coefficient ($f''(0)$) and local heat transfer (Nusselt number). Graphical legends illustrate non-dimensional velocity, temperature, and concentration on the vertical axis, with the independent parameter on the horizontal axis. Figures 2, 3, and 4 illustrate the influence of the radiation parameter on velocity, temperature, and nano-additive concentration. Higher radiation values are associated with increased fluid flow velocity, driven by radiant energy absorption and subsequent temperature elevation. The rise in temperature leads to decreased fluid density, causing volumetric expansion and heightened flow velocities. Amplified radiation values can also induce higher thermal gradients, promoting convection currents that enhance fluid motion. This highlights the intricate relationship between radiant heat transfer and fluid dynamics, emphasizing radiation's role in driving changes in fluid velocity through thermal effects. The phenomenon of increased radiation correlating with temperature

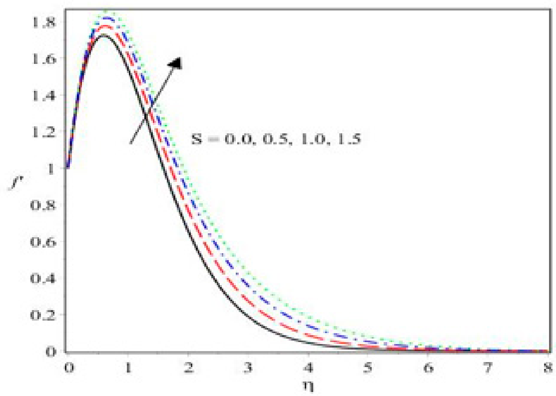

Figure 2. Impact of radiation on velocity.

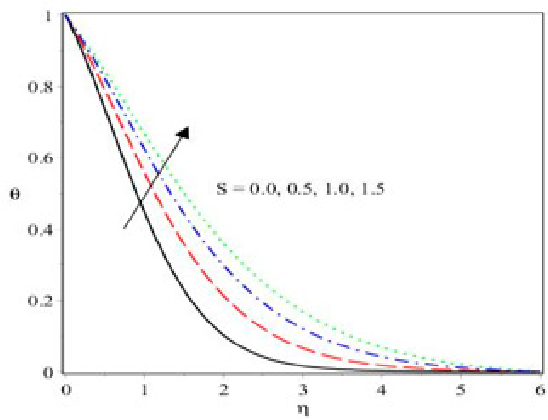

Figure 3. Impact of radiation on temperature.

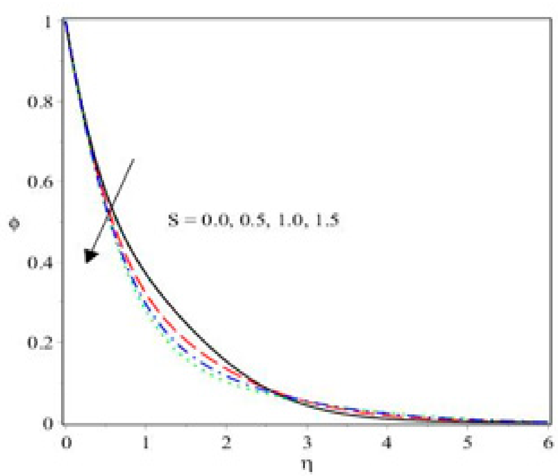

Figure 4. Impact of radiation on concentration.

rise and concentration decline can be explained by heat transfer and mass transport principles. Elevated radiation values result in more radiant energy absorption, converting into heat, impacting the fluid's temperature, and influencing nano-additive concentration through increased molecular activity and potential acceleration of chemical reactions.

Higher temperatures enhance nano-additive diffusion rates, facilitating more effective distribution and lowering overall concentration. The correlation between increased radiation values, elevated temperature, and reduced concentration underscores the intricate coupling of thermal and mass transfer processes in fluid dynamics.

The impact of the Hartmann number (H) on the system, as shown in Fig. 5, reveals that a higher H signifies stronger magnetic forces relative to fluid viscosity and conductivity in MHD flows, leading to magnetic damping and a decrease in fluid motion with increasing H. Figure 6 depicts the influence of the surface condition parameter, with increased surface roughness correlating with reduced velocity due to heightened frictional resistance, turbulence, and energy losses. Irregular surface conditions result in disruptions like vortices and eddies, reducing overall fluid velocity, while increased roughness thickens the boundary layer and impedes higher fluid velocities. A higher surface condition parameter negatively impacts fluid flow velocities by introducing resistance and disturbances in the flow field.

The application of a temperature gradient induces thermo-migration, and the Lorentz force propels the movement of nano-additives, generating electrical currents and Joule heating, resulting in a temperature rise. Nr, influenced by the Lorentz force, leads to specific particle motion based on charge and kinesis, causing concentration gradients. Higher Nr triggers electrical currents, contributing to temperature rise (Joule heating) and decreasing concentration due to preferential migration of charged species. The interplay of electromagnetic effects with heat and mass transfer processes introduces complexity to fluid dynamics, yielding unique phenomena in MHD systems.

Figure 7 depicts the influence of thermal Grash of (Gr) numbers on velocity, where increased Gr indicates stronger buoyancy forces over viscous forces, enhancing natural convection currents in the fluid. In fluid dynamics and heat transfer, higher Gr generally leads to increased fluid velocity as larger buoyancy forces intensify natural convection currents, promoting more efficient heat transfer. Figures 8 and 9 display the effect of the pedesis factor, Nb, on temperature and nanoparticle concentration,

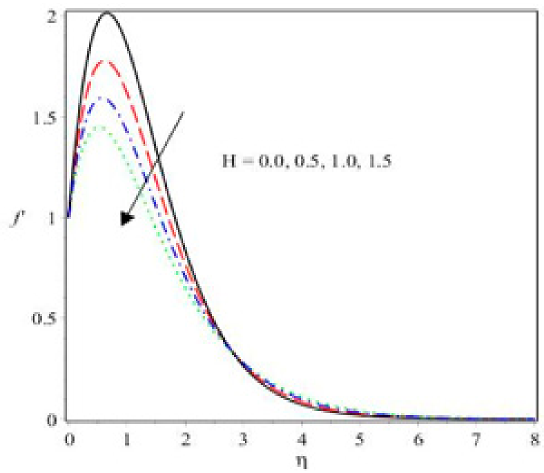

Figure 5. Impact of the Hartmann number on velocity.

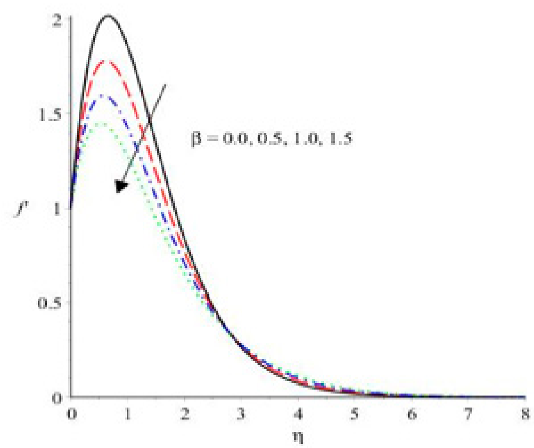

Figure 6. Impact of surface condition constraint on flow.

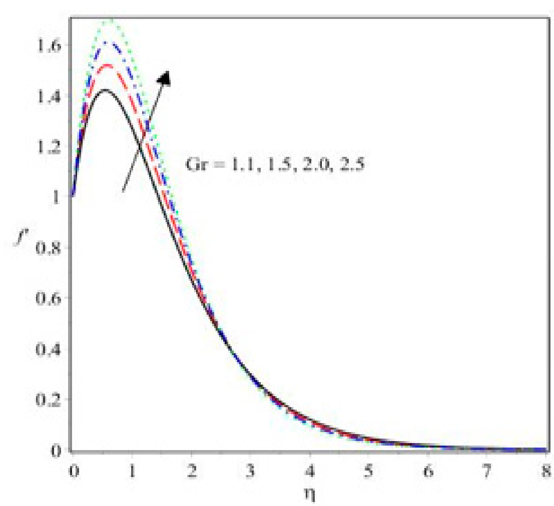

Figure 7. Impact of local thermal Grashof parameter on velocity.

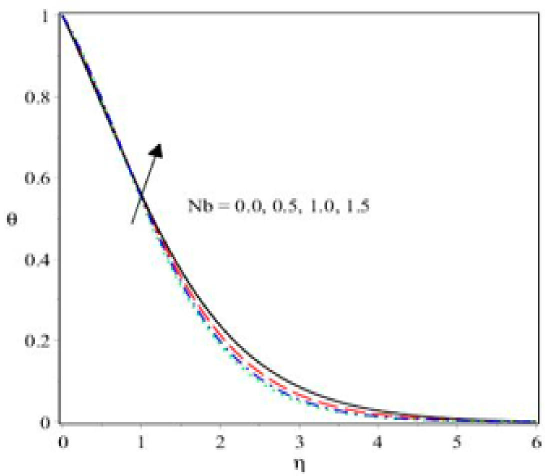

Figure 8. Impact of pedesis factor on temperature.

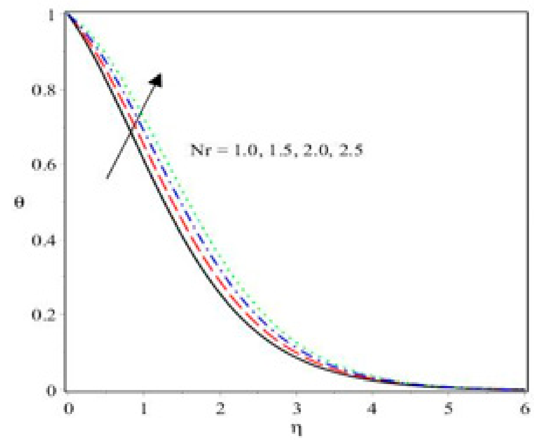

Figure 10. Impact of thermo-migration number on temperature.

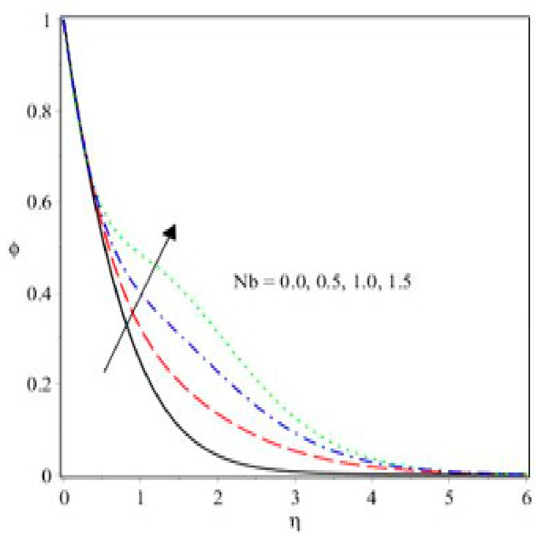

Figure 9. Impact of pedesis factor on concentration.

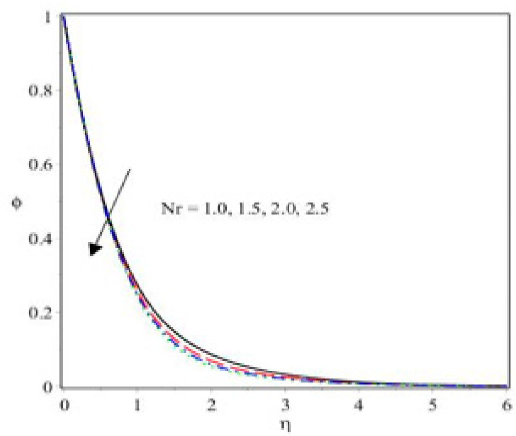

Figure 11. Impact of thermo-migration number on concentration.

respectively, where *Nb* represents random particle motion due to thermal energy transfer, enriching the fluid's thermal energy and promoting higher diffusion rates, thereby increasing nanoparticle concentration.

Figures 10 and 11 illustrate the influence of the thermo-migration parameter, *Nr*, on temperature and concentration, respectively, where *Nr*, as a fluidic parameter in MHD, is influenced by the Lorentz force resulting from the interaction between the magnetic field and the electrically conducting fluid. The application of a temperature gradient induces thermo-migration, and the Lorentz force propels the movement of nano-additives, generating electrical currents and Joule heating, resulting in a temperature rise. *Nr*, influenced by the Lorentz force, leads to specific particle motion based on charge and kinesis, causing concentration gradients. Higher values of *Nr* trigger electrical currents, contributing to temperature rise (Joule heating) and decreasing concentration due to preferential migration of charged species. The interplay of electromagnetic effects with heat and mass transfer processes introduces complexity to fluid dynamics, yielding unique phenomena in MHD systems.

Figure 12 explains the evolution of the Prandtl number, *Pr*,, with temperature in a fluid, where an increased cap P r signifies slower heat conduction and a thicker thermal boundary layer, reducing heat transport efficiency. Figure

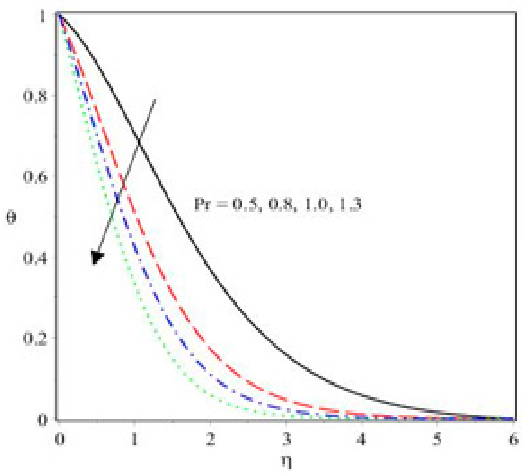

Figure 12. Impact of Prandtl number on temperature.

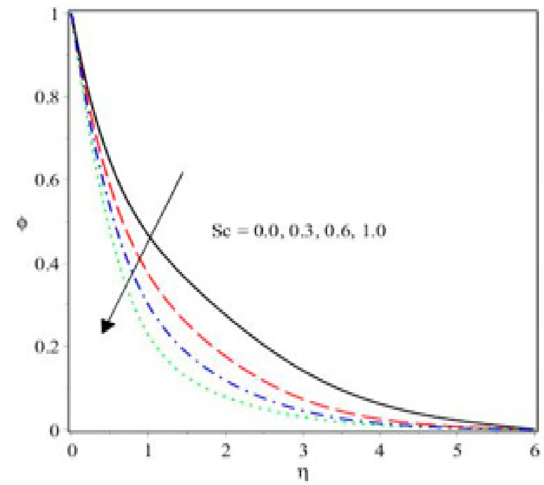

Figure 14. Impact of Schmidt factor on concentration.

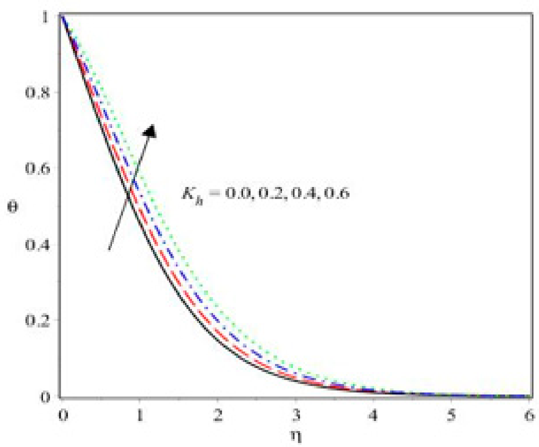

Figure 13. Impact of optimized heat parameter on temperature.

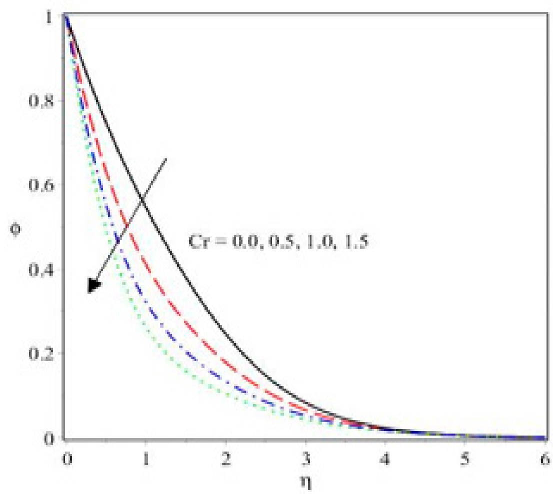

Figure 15. Impact of the generic chemical reaction rate on concentration.

13 depicts the impact of the heat generation parameter, k_h, on temperature, with an escalation intensifying heat generation within the system due to external or internal processes. Figure 14 demonstrates the influence of the Schmidt number, Sc, on nano-additive concentration, where a higher Sc leads to slower concentration diffusion, resulting in a thicker boundary layer and decreased concentration. Figure 15 shows the effect of the chemical reaction rate, Cr on concentration, with higher rates accelerating reactant depletion and producing sharper concentration gradients in MHD fluid flow, highlighting the intricate relationship between chemical kinetics, fluid dynamics, and electromagnetic interactions.

Table 1. Comparison of results for $-f''(0)$ and $-\theta'(0)$ at $Sc = 1.5$, $Pr = 0.71$, $Gr = 2.5$, $Nr = R = Q = \beta = 0.5$, $Gc = C = 0.0$.

H	Values of skin friction and Nusselt number			
	Animasaun et al. 16]	Present Result	Animasaun et al. [16]	Present Result
0.4	- 0.6085907	- 0.4380091	0.1696756	0.2690684
0.6	- 0.6368177	- 0.5725189	0.1655308	0.2417458
0.8	- 0.6637351	- 0.7184364	0.1618492	0.2147678

The Hartmann number (H) is a dimensionless parameter indicating magnetic field strength in MHD, where an increase in H signifies a stronger magnetic field, leading to augmented Lorentz forces that impede fluid motion. In boundary layer flow, an intensified magnetic field strength restricts fluid movement near the surface, causing a reduction in the skin friction coefficient, indicating decreased resistance to fluid motion. The Lorentz forces, influenced by the magnetic field, act as a damping mechanism, diminishing the velocity gradient at the fluid-solid interface. As H increases, the disrupted convective heat transfer within the boundary layer leads to suppressed thermal transport near the surface, resulting in a decrease in local heat transfer rates. The observed reduction in local heat transport underscores the intricate interplay between magnetic effects and fluid dynamics, highlighting the role of H in modulating convective heat transfer characteristics in MHD flows.

Conclusions

The study of the impact of nano-additives and generic chemical reactions on thermo-migration in high-speed MHD stream flow reveals complex interactions governing heat transfer.

The key conclusions include:

1. An increase in the surface condition parameter β leads to a decline in flow velocity.
2. Heightened pedesis values increase flow velocity, temperature, and nanoparticle concentration.
3. Increased thermo-migration Nr intensifies temperature while reducing nano-additive concentration.
4. Variations in the Hartmann number H significantly affect boundary layer thickness and the skin friction coefficient and local heat transport.
5. The combination of nano-additives and generic chemical reactions exhibits multilayered impacts on thermo-migration, emphasizing the intricate nature of high-speed MHD fluid flow phenomena.

Conflict of Interest

The authors do not have any conflicts of interest to declare.

Funding

The authors did not receive any sponsorship to carry out the research reported in the present manuscript.

Acknowledgement

The authors wish to acknowledge Prof. (Late) Ekaka-a E. N. for his constructive input which led to the success of this study.

References

Animasaun, I.I., Adebile, E.A., and Fagbade, A. I. (2016). Casson fluid flow with variable thermo-physical property along exponentially stretching sheet with suction and exponentially decaying internal heat generation using the homotopy analysis method. *Journal of Nigerian Mathematical Society*, 35, 1-17.
https://doi.org/10.1016/j.jnnms.2015.02.001

Bejawada, S.G., and Yanala, D.R. (2021). Finite element Soret Dufour effects on an unsteady MHD heat and mass transfer flow past an accelerated inclined vertical plate.
https://doi.org/10.1002/htj.22290

Boussinesq, J. (1877). Analytical Theory of Heat. *Gauthier-Villars*. *Pari*.

Farhad, A., Ilyas, K., Sheridan, S., and Norzieha, M. (2013). Heat and Mass Transfer with Free Convection MHD flows past a Vertic-al Plate Embedded in a Porous Medium. *Mathematical problems in Engineering*. Article ID 346281, 13 pages.
https://doi.org/101155/2013/346281

Goud, B.S., Kumar, P. P., and Malga, B. S. (2020). Effect of Heat source on an unsteady MHD free convection flow of Casson fluid past a vertical oscillating plate in porous medium using finite element analysis. *Partial Differential Equations in Applied Mathematics,* 2, 10001.
https://doi.org/10.1016/j.padiff.2020.100015

Jamshed, W., Eid, M. R., Nisar, K. S., Nasi, N. A. A. M., Edacherian, A., Saleel, C.A., and Vijayakumar, V. (2021). A numerical frame-work of magnetically driven Powell-Eyring nanofluid using single phase model. *Scientific Reports*.
https://doi.org/10.1038/s41598-021-96040-0

Krishna, M.V., Ahamad, N.A., and Chamkha, A.J. (2023). Hall and ion slip effects on unsteady MHD free convective rotating flow through asaturated porous medium over an exponentially accelerated plate. *Alexandria Engineering J*, 59, 565-577.
https://doi.org/10.1016/j.aej.2020.01.043.

Wakif, A., Chamkha, A., Animasaun, I. L., Zaydan, M., Waqas, H., and Sehaqul, R. (2020). Novel physical insights into the thermodynamic irreversibility within dissipative EMHD fluid flows past over a moving horizontal Riga plate in the coexistence of wall suction and joule heating effects: A comprehensive numerical investigation. *Arabian Journal for Science and Engineering*.
https://doi.org/10.1007/s13369-020-04757-3

Krishna, M.V., Ahamad, N. A., and Chamkha, A.J. (2020). Hall and ion slip effects on unsteady MHD free convective rotating flow of heat generating/absorbing second-grade fluid. *Alexandria Engineering Journal*, 60(1), 845-858.
https://doi.org/10.1016/j.aej.2020.10.013

Kumar, K.G., Reddy, M.G., Sudharani, M.V.V.N.L., Shehzad, S.A., and Chamkha, A.J. (2019). Cattaneo-Christov heat diffusion phen-omenon in Reiner-Philippoff fluid through a transverse magnetic field. *Physica A*.

Kasmani, R.M., Sivasankaran, S., Bhuvaneswari, M., and Siri, Z. (2016). Effect of chemical reaction on convective heat transfer of bound-ary layer flow in Nanofluid over a wedge with heat generation/absorption and Suction. *Journal of Applied Fluid Mechanics*, 9(1), 379-393.

Raptis, A. (2017). Effects of Thermal Radiation on the MHD Flow Past a Vertical Plate. *Journal of Engineering thermos-physics*, 26(1), 53-59.

Radouane, F., Jamshed, W., Devi, S.S. U., Prakash, M., Nisar, K.S., Nisar, A.A.M., Khashan, M.M., Yahia, I.S., and Eid, M.R. (2021). Galerkin finite element study for mixed convection ($Ti0_2 - Si0_2/water$) hybrid-nanofluid flow in a triangular aperture heated beneath. *Scientific Reports*.
https://doi.org/10.1038/s41598-021-02216-z

Rosseland, S. (1936). Theoretical Astrophysics. *Clarendon Press*, *Oxford*.

Shahzad, F., Baleanu, D., Jamshed, W., Nisar, K. S., Eid, M.R., Safdar, R., and Ismail, K.A. (2021). Flow and heat transport phenom-enon for dyamics of Jeffrey nanofluid past a stretchable sheet subject to Lorentz force and dissipation effects. *Scientific Reports*.
https://doi.org10.1038/s41598-021-02212-3

Srinivasulu, T., and Goud, B.S. (2020). Effect of inclined magnetic field on flow, heat and mass transfer of Williamson nanofluid over a stretching sheet. *Case study in thermal Engineering*, 23, 100819.
https://doi.org/10.1016/j.csite.2020.100819

Shankar, G.B., Srilatha, P., Bindu, P., and Krishna, Y.H. (2020). Radiation effect on MHD boundary layer flow due to an exponentially stretching sheet. *Adv. Math. Sci. J.*, 9, 10755-10761.

Uka, U.A., Agbo, K.O., Omamoke, E., Amos, E., and Keneke, E.D. (2022). Analytical and Simulation of hydromagnetic nano-fluid flow passing an inclined heated sheet. *International. Journal of Heat and Technology*, 40(6), 1386-1396.
https://doi.org/10.18290/ijht.400605